RESEARCH ARTICLE:

Human Balancing Performance Is Constrained by Passive Dynamics in a Real-World Inverted Pendulum

Running title: Human Balancing and Passive Dynamics

Laura Alvarez Hidalgo[1], & Ian S. Howard[2*]

[1]School of Engineering, Computing and Mathematics, University of Plymouth, Plymouth, United Kingdom.
ORCID ID: 0009-0002-2068-3390

[2]School of Engineering, Computing and Mathematics, University of Plymouth, Plymouth, United Kingdom.
ORCID ID: 0000-0002-6041-9669

[*]Correspondence should be addressed to: ISH: ian.howard@plymouth.ac.uk
Telephone: +44 1752 586324

Keywords: Human Balance, Inverted Pendulum, Predictive Control, Learning Transfer, Real-World Dynamics, Sensorimotor Control.

Number of pages: 23
Number of figures: 8
Number of tables: 2
Number of words for Abstract: 302
Number of words for Introduction: 559
Number of words for Discussion: 1555

Conflict of Interest

The authors declare that they have no financial, personal, or professional interests that could be construed to have influenced the paper.

AI use statement

The authors used ChatGPT solely as a general research aid for language editing and for identifying potentially relevant literature. All scientific content, interpretations, and references were selected, verified, and entered by the authors.

Abstract
Motor adaptation is typically studied with simplified virtual tasks that use an abstract representation of the mass, inertia and intrinsic instability of real objects. Here we examined how humans stabilize a real, underactuated inverted pendulum and how performance depends on the plant's passive dynamics. Twelve right-handed adults balanced a real inverted pendulum by moving a cart along a linear rail, using three different rod lengths (short 0.31m, medium 0.64m, long 1.03m). Study 1 characterized the passive mechanics of each rod using free-decay and fall-to-±30° trials following release from the upright position. Longer rods exhibited slower decay and lower natural frequencies, as well as a longer duration before falling, indicating slower passive dynamics. Study 2 assessed balance control while participants attempted to maintain stability. Human participants trained with the medium pendulum (30 trials) and were then assessed with all three pendulums (20 trials each). During training, time to failure increased significantly across trials, indicating clear learning of the medium-pendulum task. In contrast, performance during the subsequent testing blocks showed no further within-block improvement, suggesting that the main learning-related gains had already occurred during training. During testing, performance depended strongly on pendulum condition: the short pendulum was balanced for less time than the medium and long pendulums, whereas the medium and long pendulums did not differ reliably in final time to failure. Estimated peak pendulum angular velocity varied systematically with rod length, decreasing as length increased, whereas maximum cart speed differed across conditions but did not scale monotonically with rod length. This indicated that participants did not compensate for shorter, more unstable rods by producing proportionally faster cart movements. Together, these results indicate that human balancing performance was strongly constrained by the passive dynamics of the plant. The short and faster pendulum was markedly more difficult to balance than the medium and long pendulums.

Introduction

Humans continually adjust their movements to meet changing environmental and task demands. This adaptive capability, known as motor adaptation, is thought to involve the nervous system updating internal representations of the body and environment through sensory feedback and error-based learning (Shadmehr et al., 2010; Wolpert et al., 2011; Howard et al., 2013, 2017). These processes are believed to support predictive control, enabling behavior to remain effective despite noise, delays, and perturbations.

Much of what is known about motor adaptation derives from tightly controlled laboratory tasks using artificial perturbations, such as visuomotor rotations or curl field force perturbations applied to the hand (Howard et al., 2009, 2012; Franklin and Wolpert, 2011; Krakauer and Mazzoni, 2011; Taylor and Ivry, 2012). While these paradigms provide clear experimental leverage on learning mechanisms, they often minimize or eliminate key

properties of everyday interactions, such as the combined effects of mass, inertia, contact forces, and intrinsic instability. As a result, important questions remain about how humans adapt when confronted with the physical dynamics of real objects that differ in their intrinsic properties.

Balancing tasks offer an ecologically meaningful window onto such control problems. They are inherently unstable and demand the integration of feedback and predictive control to maintain equilibrium. The inverted pendulum captures core challenges of real-world control: underactuation, sensorimotor delays, and high sensitivity to small disturbances (Scott, 2004; Gawthrop and Wang, 2006; Liu and Todorov, 2007). Comparable dynamics arise in human posture, manual object manipulation, and everyday load handling (e.g., carrying a tray or a cup of tea), where success hinges on anticipating and counteracting the evolving effects of the object dynamics. Physical inverted pendulums have long served as a model system for human balance control, particularly in stick-balancing and cart-pendulum paradigms, because time-delayed feedback and the intrinsic dynamics of the plant strongly influence the temporal margin available for successful correction (Yoshikawa et al., 2016).

Many previous studies have examined balance control using simplified or virtual implementations, such as tracking a simulated pendulum or stabilizing one via a robotic interface that abstracts away mechanical complexities (Burdet et al., 2001; Mehta and Schaal, 2002; Milner and Franklin, 2005; Howard et al., 2009). These approaches help isolate specific mechanisms but often rely on artificially simulated feedback and omit important aspects of the task. By contrast, the present study uses a physical inverted pendulum task that preserves direct visual information about the pendulum and direct interaction with the forces generated by the system's dynamics. Participants stabilized a real-world inverted pendulum by manually controlling a rolling cart in an underactuated setting, in which the rod is controlled only indirectly via base motion.

Crucially, we varied pendulum length (short, medium, and long), thereby altering the passive dynamics, time constants, and stability characteristics of the plant. This design allows us to evaluate whether human balancing performance is constrained by changes in the passive dynamics of the pendulum. The design of the experiments was based on a previous pendulum rig (Alvarez Hidalgo and Howard, 2022, 2024), developed to investigate control engineering approaches to balance. Here, we used a modified version of that apparatus for two purposes: first, to characterize the passive mechanical behavior of pendulums with different lengths; and second, to quantify human balancing performance across the same pendulum conditions. This allows us to ask whether differences in passive plant dynamics are reflected in corresponding differences in active human balancing performance.

Methods

Participants

Twelve right-handed adults (8 female, 4 male; mean age = 24.67 ± 3.95 years) participated in the study. Participants were randomly assigned to one of two groups (Group A or Group B; n = 6 per group) to counterbalance the order of experimental conditions.

All participants were naïve to the purpose of the study and provided written informed consent prior to participation. Handedness was confirmed using the Edinburgh Handedness Inventory (Oldfield, 1971), which verified that all participants were right-handed. The study received ethical approval from the Faculty Research Ethics and Integrity Committee at the University of Plymouth and was conducted in accordance with institutional guidelines.

Apparatus

The experimental task was implemented using a custom-built inverted pendulum apparatus mounted on a standard-height desk (Fig. 1), similar to that described in prior work (Alvarez Hidalgo and Howard, 2022, 2024). The system consisted of a rigid horizontal frame supporting a rolling cart that moved along the x-axis. A detachable vertical rod was attached to the cart via a pivot joint, forming an underactuated inverted pendulum, in which the rod could be controlled only indirectly through movement of the cart.

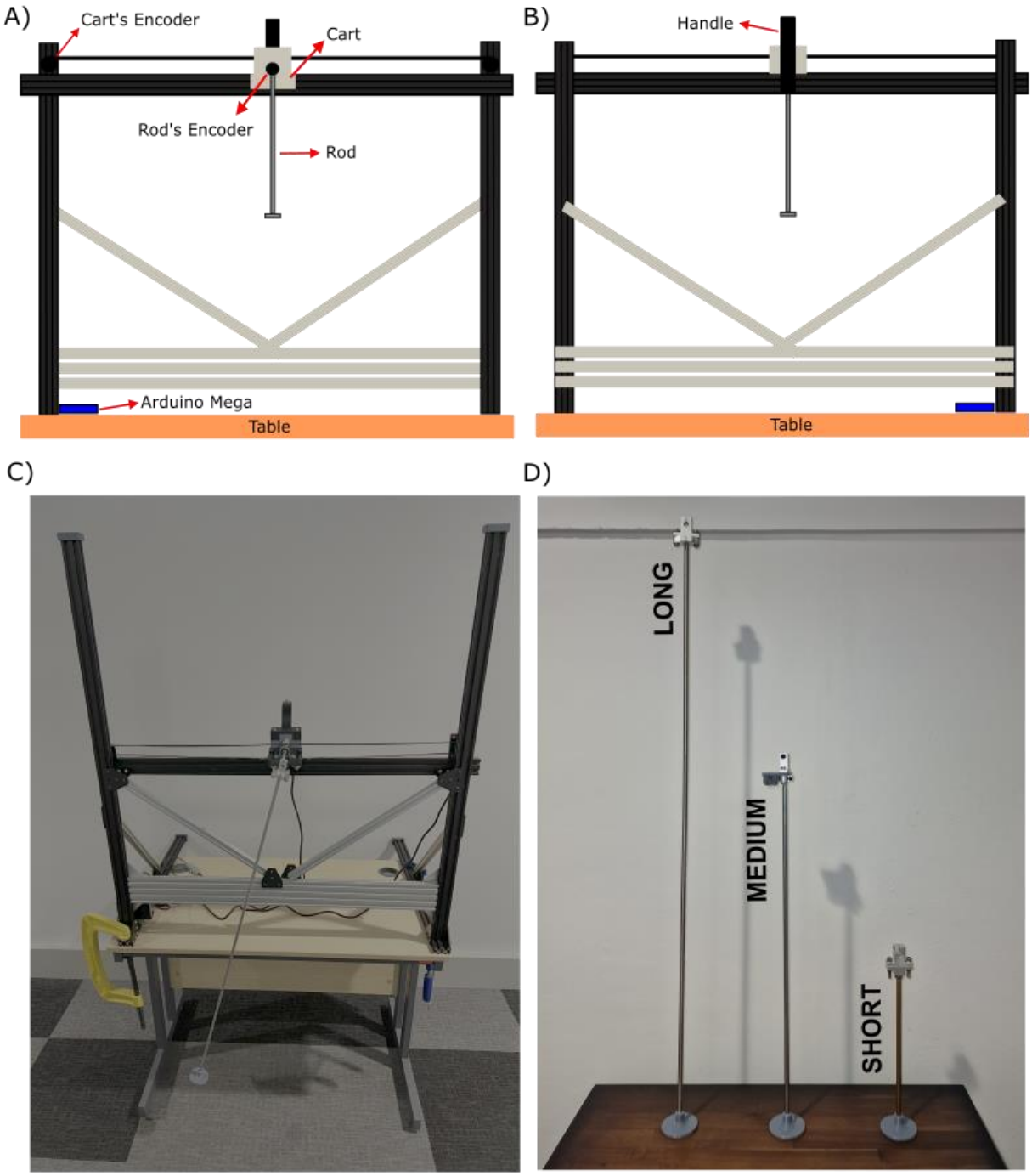

Figure 1. Schematic and photographic views of the inverted pendulum apparatus. **A)** Front view of the setup, showing the rolling cart and vertical rod assembly. **B)** Rear view, highlighting the handle used for manual control. **C)** Photograph of the complete rig mounted on a standard-height desk. **D)** The three interchangeable pendulum rods (short, medium, and long).

Motion data were recorded using two rotary encoders (2400 pulses per revolution, counted using all quadrature edges). One encoder was mounted at the end of the rail and measured horizontal cart displacement via a GT2 belt attached to the cart and a 36-tooth GT2 pulley. The second encoder was located at the rod-cart pivot and measured pendulum angle relative to the vertical. To systematically vary the pendulum dynamics, three rods of different lengths were used: a short brass rod (305 mm, 90 g), a medium stainless-steel rod (635 mm, 143 g), and a long stainless-steel rod (1030 mm, 216 g). All rods shared the same 8 mm diameter and mounting interface to ensure consistent mechanical coupling with the cart.

Table 1. Mechanical properties of the three inverted pendulum rods.

		Short Pendulum	**Medium Pendulum**	**Long Pendulum**
Length (L)	[m]	0.31	0.64	1.03
Mass (m)	[kg]	0.09	0.14	0.22
Distance from pivot to center of gravity	[m]	0.15	0.32	0.52
Weight (W)	[N]	0.88	1.40	2.12
Estimated Moment of Inertia around center of gravity (I_{cog})	[kg·m^2]	0.0007	0.005	0.02

Participants controlled cart position via a rear-mounted handle. The entire rig was securely clamped to the desk to maintain mechanical stability. An Arduino Mega 2560 microcontroller logged pendulum angle and cart position at approximately 10 Hz, with each sample stored together with a precise timestamp. For analysis and display, the recorded signals were then interpolated to 100 Hz. Velocity measures were subsequently estimated from these timestamped position signals and should therefore be interpreted as approximate rather than high-precision kinematic measurements.

Experimental Setup

Two complementary studies used the same inverted pendulum apparatus (Fig. 1). Auditory tones cued the start and stop of a trial. Study 1 quantified passive mechanical dynamics without human input. Study 2 examined human balance control while

participants attempted to stabilize the inverted pendulum. The same trial termination threshold was used in both studies: trials ended when the pendulum angle exceeded ±30°.

Study 1: Passive System Identification

To characterize the dynamic properties of the inverted pendulum system, we conducted a set of trials without human control, designed to capture the passive dynamics and to quantify how each pendulum length affected stability and subsequent decay behavior. For each pendulum length, we recorded data using two passive protocols.

The first protocol examined full passive decay; and a single trial for each pendulum length was recorded. The rod was released from the upright position and allowed to move freely until motion ceased, yielding a continuous decay trajectory. For this protocol, the upright position corresponded to 180°; the rod then moved away from the unstable upright position and eventually decayed toward the downward resting position near 0°.

The second protocol used a passive fall-to-±30° procedure. Here, the rod was manually raised to the upright position and released to fall freely. The trial ended when the pendulum angle reached ±30°, matching the failure threshold later used in Study 2. To obtain a more reliable estimate of the effect of pendulum length on passive fall behavior, 20 trials were collected for each pendulum length.

Because the initial release was performed manually, some variability in initial angle and initial angular velocity was unavoidable. In addition, small uncontrolled environmental disturbances, such as air currents, may have contributed modest trial-to-trial variability.

Study 2: Human Study of Balance

Prior to the start of the human experiment, participants were instructed to move the cart left and right while holding the handle of the rig. They were also told to focus their gaze on the top of the rod throughout the trials, and to begin moving upon hearing a “beep” and to stop moving upon hearing a second “beep.”

During each trial, participants held the handle attached to the cart. When the participant was ready, the researcher slowly raised the pendulum rod from its initial resting position towards the vertical. When the pendulum’s angular velocity, as measured by the encoder, fell below 5 $deg \cdot s^{-1}$, a 3-second auditory tone (400 Hz) was presented. The encoder count was then reset to zero, defining the upright position of the pendulum as 0°, which provided the reference point for the experiment.

Participants then attempted to balance the inverted pendulum. Each trial ended either when the rod angle exceeded ±30°, or when the participant successfully maintained balance for 10 seconds. Time to failure was therefore defined as the time until the

pendulum exceeded ±30°, or the full 10 s trial duration if balance was maintained successfully throughout the trial. At the conclusion of each trial, another 3-second auditory tone was played to signal trial end to both the participant and the researcher.

Participants did not receive any formal feedback on their performance, aside from being able to observe how long they had balanced the pendulum. No scheduled breaks were provided during the experiment, apart from the brief pauses between trials. Participants also rested briefly during changes in pendulum length.

Each participant completed one training block followed by three testing blocks (Fig. 2). During the training block, participants always used the medium-length inverted pendulum and completed a total of 30 trials.

After training, participants proceeded to the testing phase, beginning with 20 trials using the same medium-length rod. They then completed 20 trials each with the remaining two rod lengths: the short and the long inverted pendulum. The order in which participants performed the short and long rod testing phases was counterbalanced across participants to control for potential order effects. Thus, participants were assigned to one of two testing orders: medium-short-long or medium-long-short.

Each testing block consisted of 20 consecutive trials using a single rod length. In total, each participant completed 90 trials: 30 during the training phase and 60 during the testing phases (20 per rod length). The entire experiment took approximately 60 minutes to complete per participant.

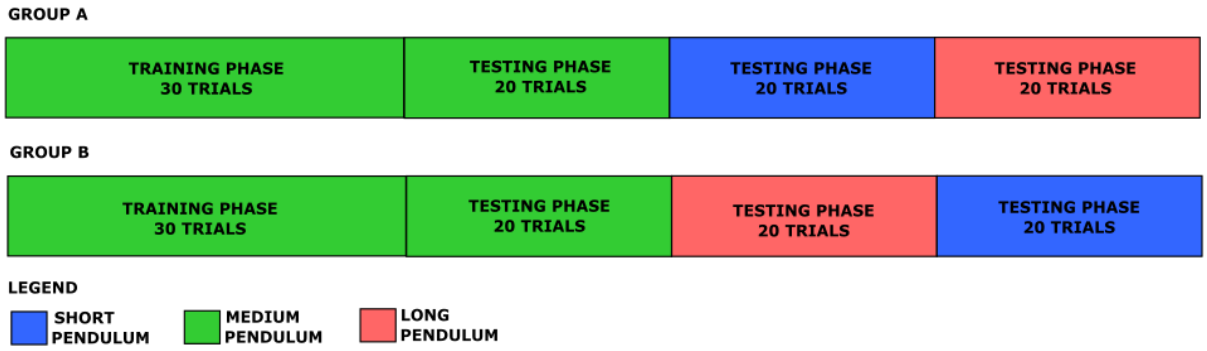

Figure 2. Experimental design and trial structure across conditions. Each row shows the sequence of phases for each group. All participants trained with the medium rod (30 trials; green), then completed testing phases (20 trials each) with the medium rod first, followed by the short (blue) and long (red) rods in counterbalanced order. Thus, one group completed the order medium-short-long, whereas the other completed medium-long-short.

Measurements

The rotary encoders provided time-indexed measurements of cart motion and pendulum angle. Cart position, $x(t)$, was computed from cart encoder counts by mapping shaft rotation to linear translation through the GT2 timing-belt transmission. Cart velocity was estimated from the interpolated encoder position signals and reported in meters per second ($m \cdot s^{-1}$). Pendulum angle, $\theta(t)$, was recorded at the pivot encoder and zeroed at the upright position, such that $\theta = 0°$denoted the unstable equilibrium.

Rod-Specific Mechanical Parameters

To characterize the pendulums, the following mechanical properties were measured or calculated:

Length (L): Distance from pivot to tip, in meters.

Mass (m): Measured using a balance in kg.

Distance from pivot to center of gravity (l): For a uniform rod, this was assumed to be half the rod length.

$$l = \frac{L}{2} \tag{1}$$

Moment of Inertia (I_{cog}): A measure of the rod's resistance to angular acceleration about its center of gravity, in $kg \cdot m^2$.

$$I_{cog} = \frac{1}{12} m \cdot L^2 \tag{2}$$

Weight (W): The gravitational force acting on a body's mass, in Newtons.

$$W = m \cdot g \tag{3}$$

These parameters can be used to derive linearized dynamics for the corresponding pendulum model. The small-angle natural frequency of this model is:

$$f_0 = \frac{1}{2\pi} \sqrt{\frac{mgl}{I_{cog} + ml^2}} \tag{4}$$

where $l = L/2$ denotes the distance from the pivot to the center of gravity. Natural frequency, f_0, is the intrinsic undamped oscillation rate of the linearized pendulum model. This expression was used to characterize the expected passive dynamics of the pendulum, alongside the empirical passive measurements reported in Study 1.

Angle-based kinematics

To characterize the kinematics of the system, pendulum angle and angular velocity, as well as cart position and linear velocity, were calculated. For real-time operation on the microcontroller, velocity estimates were required to determine whether the rod was stationary at the beginning of each trial. These real-time estimates were obtained by differencing encoder counts and scaling them appropriately. Cart velocity, $v_{\mathrm{cart}}(t)$, was obtained from cart encoder counts and converted to meters per second via the GT2 belt transmission. Pendulum angular velocity, $\dot{\theta}_{\mathrm{pend}}(t)$, was obtained from the encoder-measured pendulum angle after converting counts to angle in degrees and applying wraparound correction.

$$v_{Cart}\ (t) = \frac{dx_{Cart}(t)}{dt} \tag{5}$$

$$\dot{\theta}_{Pend}\ (t) = \frac{d\theta_{Pend}(t)}{dt} \tag{6}$$

For offline analysis, higher-resolution signal processing was used. The recorded encoder position signals were first interpolated to a regular sampling frequency of 100 Hz using the MATLAB ***interp1*** command with the spline option. Pendulum and cart velocities were then estimated using the MATLAB ***gradient*** command rather than a simple first-difference operator. This interpolation also provided a more temporally resolved estimate of the time at which the pendulum passed the ±30° threshold, compared with using only the first raw sample that exceeded this value.

Outcome measures aligned to Results

Time to failure was defined as the duration from trial onset to trial termination. Trials ended either when the absolute value of the pendulum angle exceeded 30°, or when the participant successfully maintained balance for a maximum of 10 s. Accordingly, time to failure was capped at 10s for successfully completed trials. This measure reflects the participant's ability to stabilize the system over time.

$$t_{30} = t_{end} - t_{start} \tag{7}$$

Approximate peak velocity was defined as the maximum estimated absolute speed attained during a trial at the respective encoder. During offline analysis, peak cart velocity was calculated as an approximate indicator of the maximum cart motion generated during balancing, whereas peak pendulum angular velocity provided a corresponding measure of rod motion. Because velocities were derived from low-frequency position recordings,

they should be interpreted as approximate descriptive kinematic measures rather than high-precision velocity estimates.

Results

This section covers the dynamic properties of the pendulum system and the behavioral outcomes across both passive and active balancing conditions. We first describe the findings from Study 1, which quantified passive decay and fall dynamics in the absence of human control. We then present the main behavioral results from Study 2, including changes in time to failure across training and testing phases, as well as estimated peak velocity metrics for both the cart and pendulum. Where appropriate, statistical comparisons are based on repeated-measures ANOVAs with post hoc corrections, and all reported effects are accompanied by descriptive statistics and standard error estimates.

Study 1: Passive System Identification

Free Decay

Total decay time following release increased monotonically with rod length. The short rod reached near-zero motion after 100.1 s, whereas the medium rod decayed after 240.1 s, and the long rod took approximately 300.1 s to settle. These durations reflect the increasing moment of inertia of the longer pendulums and the correspondingly smaller angular acceleration produced by gravity for a given angular displacement, which prolongs the passive dynamics and increases the time required for motion to decay in the absence of external control.

The oscillation frequency showed the inverse pattern, again consistent with slower passive dynamics in the longer pendulums: the long pendulum oscillated at 0.59 Hz (period = 1.71 s), the medium at 0.74 Hz (period = 1.35 s), and the short at 1.05 Hz (period = 0.95 s). Fig. 3 shows the measured decay durations and representative angular trajectories for each condition.

Fall to ±30°

Fall time from upright to the ±30° threshold increased consistently with rod length, again in line with the slowing of passive dynamics as pendulum length increased. To characterize the effect of pendulum length on passive fall behavior within this experimental setup, time to failure was examined across three conditions: short, medium, and long pendulums. Each trial was terminated when the pendulum reached an angular displacement of ±30°, which defined the failure threshold under passive dynamics. Because the dataset comprised 20 repeated drops of the same apparatus performed by the same operator, these trials were treated as repeated observations within a single setup rather than as independent subject-level replicates.

Descriptive statistics are reported in Table 2. Mean time to failure increased from 1.13 s in the short condition to 1.37 s in the medium condition and 1.44 s in the long condition, indicating that longer pendulums took longer to reach the ±30° threshold.

An exploratory within-setup comparison indicated an overall difference across conditions (Welch's ANOVA: $F(2,37.07) = 6.60$, $\omega^2 = 0.138$, $p = .004$). Games–Howell post hoc comparisons showed that the short pendulum had a significantly shorter time to failure than both the medium ($p = .018$) and long ($p = .009$) pendulums, whereas the medium and long conditions did not differ significantly ($p = .770$). However, these statistical comparisons should be interpreted only as characterizing repeated behavior of this specific apparatus and release procedure, rather than as population-level inference.

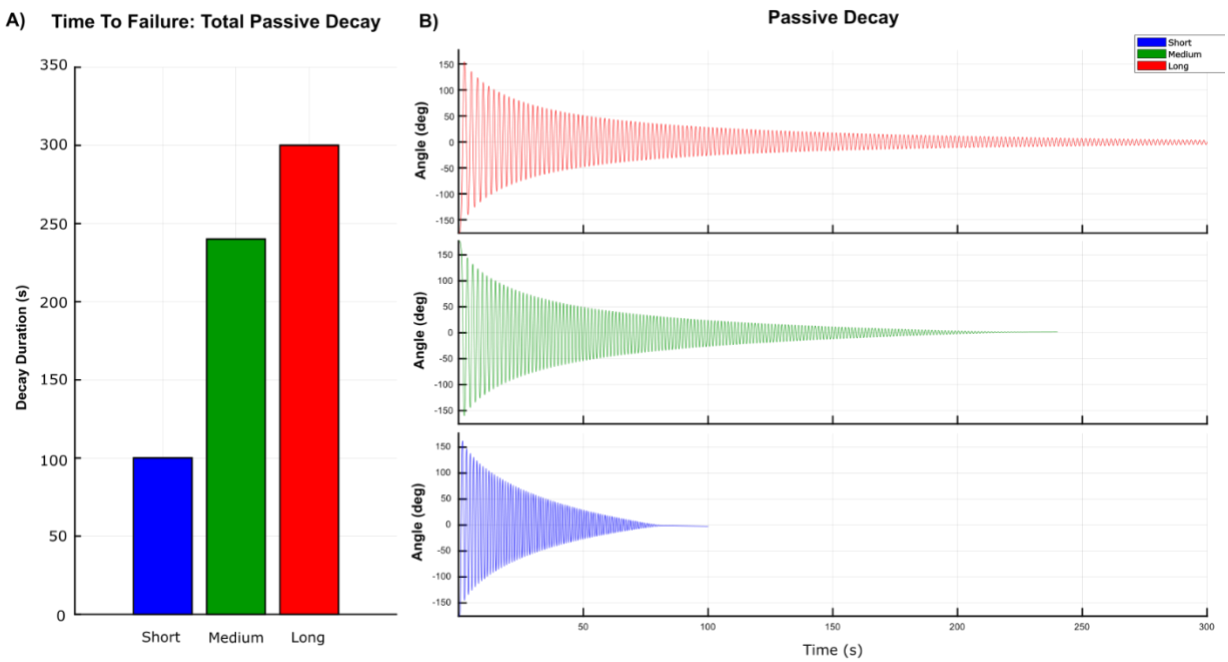

Figure 3. Passive free-decay dynamics for the three rod lengths. A) Overall decay time per rod length. B) Angular pendulum trajectories as a function of time for the unassisted free-decay experiments.

Table 2. Descriptive statistics for time to failure during passive falls to ±30°.

Condition	Mean Time to Failure (s)	SD	Coefficient of variation
Short	1.13	0.24	0.22
Medium	1.37	0.28	0.21
Long	1.44	0.37	0.26

Trial number was not treated as an additional experimental factor, because the repeated drops do not constitute independent repeated-measures observations in the usual inferential sense. Instead, the distribution of trial-wise values is shown in Fig. 4 to illustrate the consistency and spread of the repeated observations within each condition. Overall, these results show that, within this apparatus and manual release procedure, the short pendulum reached the ±30° threshold more quickly than the medium and long pendulums, consistent with faster passive fall dynamics for the shorter rod.

Figure 4. Time to failure for passive falls to ±30° across pendulum conditions. Individual trial data are shown for short, medium, and long pendulums, displayed with horizontal jitter for clarity. Black squares indicate the condition means, and error bars denote ±SE.

Study 2: Human Study of Balance

Time to Failure Across Training and Testing Blocks

As shown in Fig. 5, participants improved substantially during the initial training phase with the medium-length pendulum. To quantify this, participant means were calculated for the first four and last four trials of each block: the medium training block and the short, medium, and long testing blocks. These data were analyzed using a mixed repeated-measures ANOVA with Block (Medium Training, Short, Medium Testing, Long) and Phase (Start, End) as within-subject factors, and Order as a between-subject factor.

There was a significant main effect of Block, $F(3,30) = 47.65,\ p < .001,\ \omega^2 = 0.551$, a significant main effect of Phase, $F(1,10) = 15.42,\ p = .003,\ \omega^2 = 0.064$, and, crucially, a significant Block × Phase interaction, $F(3,30) = 5.75,\ p = .003,\ \omega^2 = 0.073$. No effects involving Order reached significance (all $p \geq .298$), indicating that performance did not depend on presentation order. Mauchly's tests were not significant for either Block or Block × Phase, so sphericity was not considered violated.

The Block × Phase interaction reflected improvement occurring primarily during the medium training block. Mean time to failure increased from 2.17 ± 0.78 s at the start of training to 4.33 ± 1.83 s at the end of training, and this change was significant ($p = .009$). In contrast, there was no significant start-to-end change within the short test block (1.92 ± 0.52 s to 2.01 ± 0.59 s, $p = 1.000$), the medium test block (4.95 ± 2.26 s to 5.73 ± 2.10 s, $p = .462$), or the long test block (6.45 ± 2.06 s to 6.33 ± 2.52 s, $p = 1.000$).

These results indicate that the main learning-related improvement in balancing performance occurred during the initial medium-pendulum training phase, whereas performance during the subsequent testing blocks remained relatively stable.

Final Time to Failure Across Pendulum Length Conditions

To assess stabilized performance after the initial training-related improvement, time to failure was compared across pendulum lengths using the mean of the final four trials from each testing block. As shown in Fig. 6A, mean time to failure was 2.01 s for the short pendulum, 5.72 s for the medium pendulum, and 6.30 s for the long pendulum. A one-way repeated-measures ANOVA confirmed a significant main effect of condition on time to failure, $F(2,22) = 33.15, p < .001, \omega^2 = 0.488$. Bonferroni-corrected post hoc comparisons showed that participants balanced the short pendulum for significantly less time than both the medium and long pendulums (both $p < .001$); the medium and long pendulum conditions did not differ significantly ($p = .76$).

When order group was included as a between-subject factor (Fig. 6B), the main effect of condition remained significant, $F(2,20) = 31.38, p < .001, \omega^2 = 0.496$. There was no significant main effect of Order, $F(1,10) = 0.23, p = .642, \omega^2 = 0.000$, nor Condition × Order interaction, $F(2,20) = 0.178, p = .831, \omega^2 = 0.000$. Thus, the effect of pendulum length on final balancing performance was robust to the order in which the conditions were experienced.

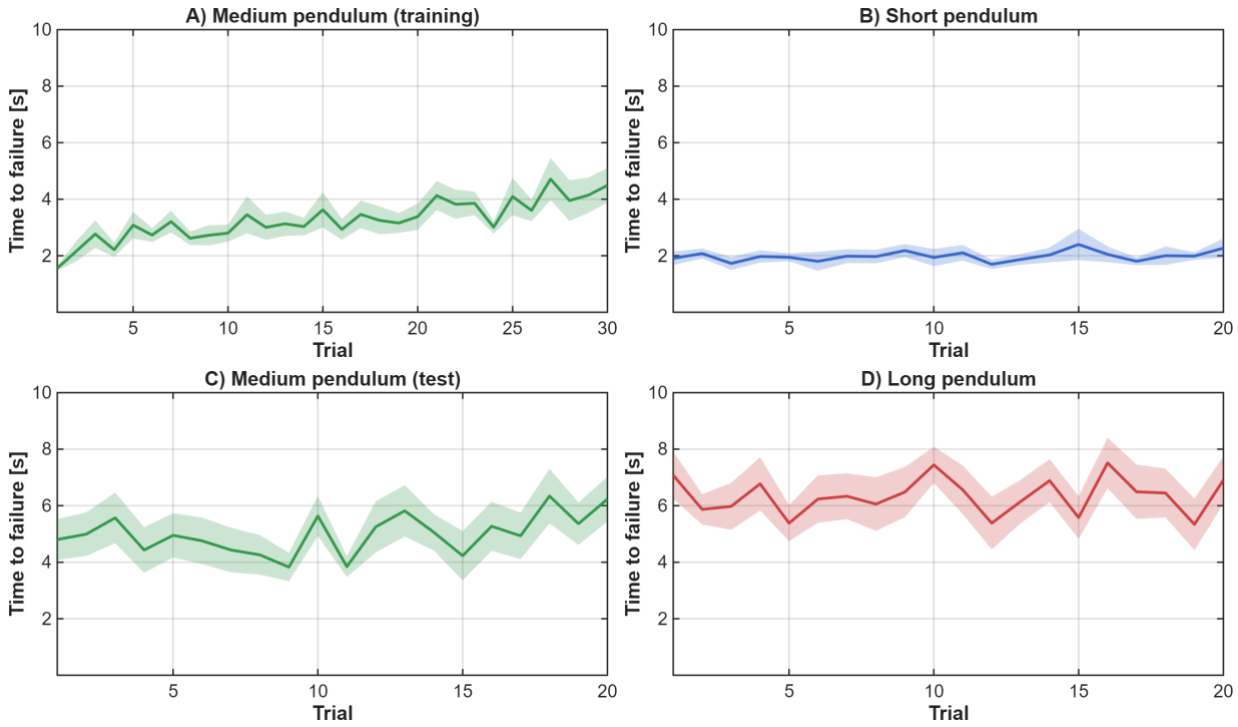

Figure 5. Time to failure across human participants and across trials. **A)** Trial times during the medium-length pendulum training phase. **B)** Time to failure during the testing short pendulum condition. **C)** Time to failure during the testing medium pendulum condition. **D)** Time to failure during the testing long pendulum condition.

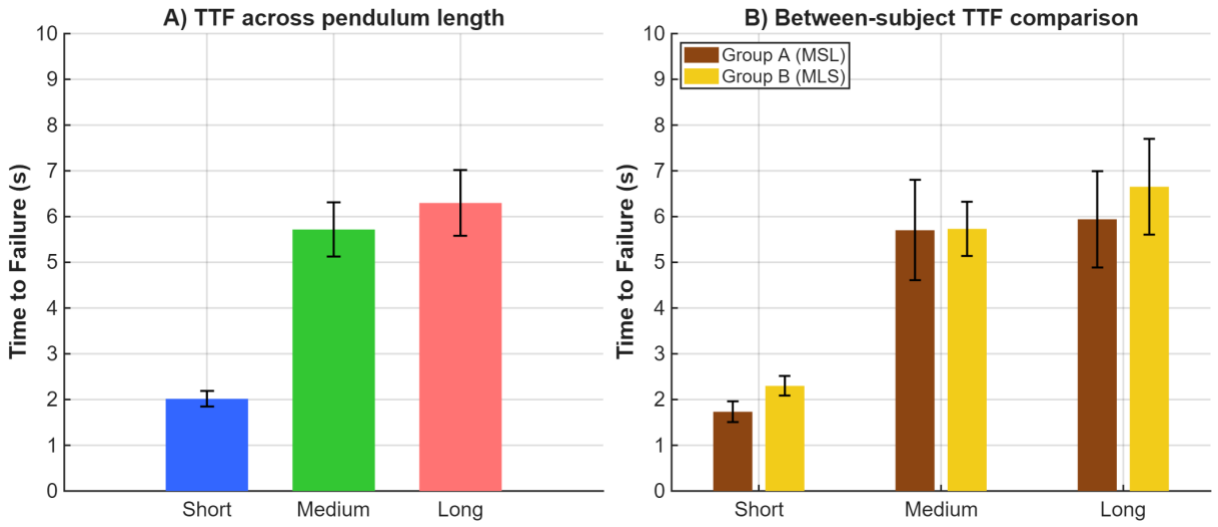

Figure 6. Time to failure across human participants during the last 4 trials. **A)** Time to failure across each pendulum length condition. **B)** Between-subject comparison of mean time to failure for each pendulum length condition.

Peak Cart and Rod Velocities

To better understand how participants adapted their control strategies across pendulum conditions, we estimated peak cart velocity and peak pendulum encoder angular velocity during the final four trials, when behavior had stabilized. Because these velocities were derived from low-frequency sampled position data, they should be interpreted as approximate descriptive measures rather than precise estimates.

Estimated peak pendulum angular velocity varied systematically with rod length (Fig. 7B). A repeated-measures ANOVA revealed a main effect of condition, $F(2,22) = 48.06, p < .001, \omega^2 = 0.67$. Angular velocities were highest for the short condition (220.2 ± 35.21 deg·s⁻¹), intermediate for the medium condition (157.2 ± 34.36 deg·s⁻¹), and lowest for the long condition (97.47 ± 33.15 deg·s⁻¹). Pairwise comparisons confirmed significant differences between all three conditions after Holm correction: short vs. medium ($p < .001$), short vs. long ($p < .001$), and medium vs. long ($p < .001$).

As shown in Fig. 8, maximum cart speed over the final four trials also differed significantly across pendulum length conditions. Mean maximum cart speed was 0.904 m·s⁻¹ in the short condition, 1.051 m·s⁻¹ in the medium condition, and 0.809 m·s⁻¹ in the long condition, indicating that cart speed was highest in the medium condition and lowest in the long condition. Mauchly's test did not indicate a violation of sphericity ($W = 0.588$, $\chi^2(2) = 5.302$, $p = .071$); Greenhouse–Geisser-corrected results are reported as a conservative precaution ($\varepsilon = 0.708$). The ANOVA showed a significant main effect of condition, $F(1.42,15.59) = 9.66, p = .004, \omega^2 = 0.126$. Holm-corrected post hoc comparisons confirmed that cart speed was higher in the medium than in the long condition (p = .004); the short condition also exceeded the long condition (p = .046), whereas the short and medium conditions did not differ reliably (p = .055). There was no consistent relationship between maximum cart speed and rod length.

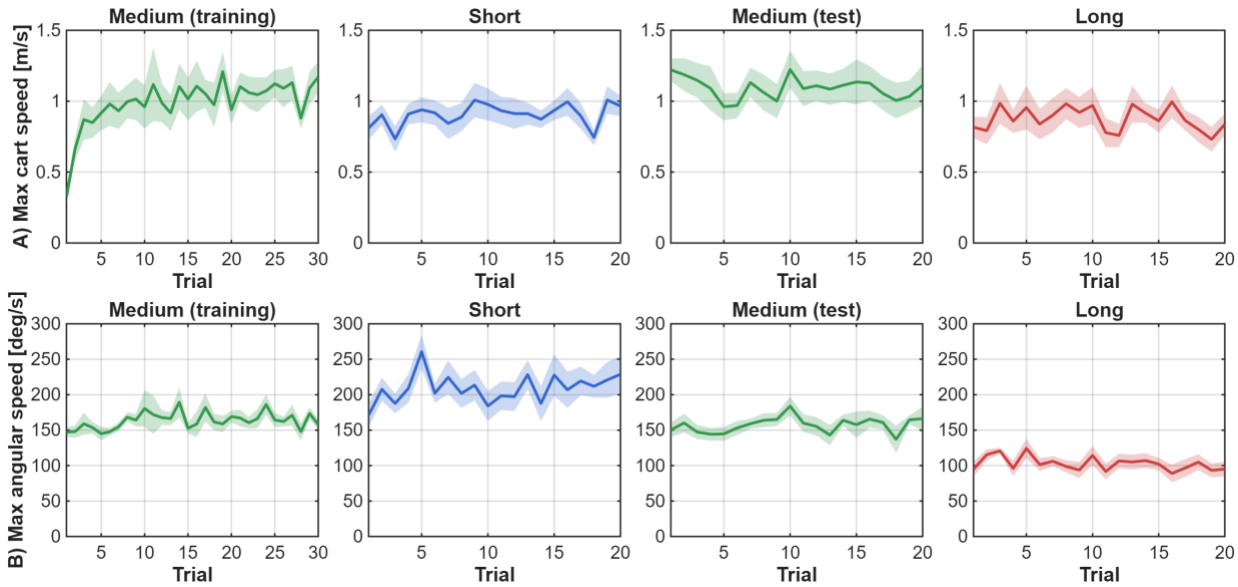

Figure 7. Peak estimated velocities for the different pendulum length conditions and experimental phases. **A)** Per trial-pair peak cart velocities. The colored line represents the group mean, with the shaded band showing ±1 standard error (SE). The x-axis indicates the trial-pair index. Velocities are computed as absolute peak values ($|\, m \cdot s^{-1} \,|$). **B)** Per trial-pair peak pendulum encoder angular velocities. Velocities are computed as absolute peak values ($|\, deg \cdot s^{-1}$). As in panel A, coloured lines show the group mean, and shaded bands denote ±SE across participants.

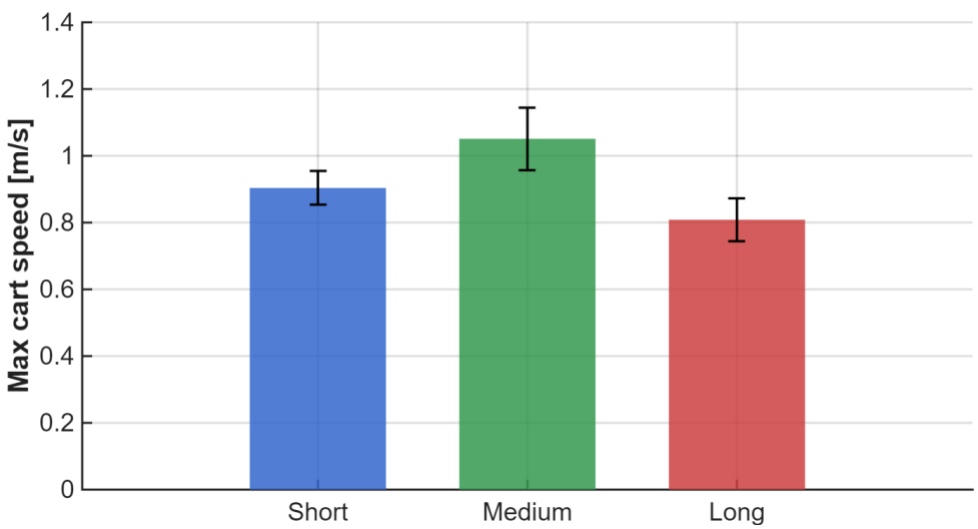

Figure 8. Maximum cart speed across human participants during the last 4 trials.

Discussion

Understanding how humans behave in real physical environments is a central question in motor control research. While most previous studies have used simplified, virtual tasks,

our study explores control in a physically unstable, real-world system. We presented a real-world balancing study showing that human balancing performance tracks passive plant dynamics and is constrained by the system's intrinsic mechanics. Specifically, we examined the manual balancing of inverted pendulums of three different lengths, with the short pendulum being markedly more difficult to balance than the medium and long pendulums. We first investigated the passive dynamics of the pendulums and then assessed the ability of human participants to balance them.

Comparative results: passive mechanics vs human control

Across both experiments, a consistent relationship emerged between the passive mechanical properties of the pendulum system and human performance during active balancing.

The passive characterization revealed that pendulum length substantially modulated the plant's intrinsic dynamics. Consistent with established physical principles, longer rods exhibited greater decay durations and lower dominant frequencies, whereas shorter rods decayed more rapidly and oscillated at higher frequencies. In the fall-to-±30° trials, the time to failure followed the same ordering, confirming that longer rods had slower passive fall dynamics and provided a larger temporal margin before reaching the failure threshold. These differences affect control difficulty, with longer rods providing greater temporal margins for correction, while shorter rods demand faster and more precise intervention to maintain stability.

Static friction at the pivot must be overcome before the pendulum rod begins to move, and its effect is proportionally greater in shorter pendulums because the available restoring torques are smaller. Although sufficiently large stiction could in principle delay motion onset in a very short pendulum, friction in the present apparatus was low and was therefore unlikely to have been a major factor in the present experiments. Once motion began, static friction was replaced by dynamic friction, introducing a nonlinearity that may have complicated control, although this effect was also likely to have been small.

An energy-based perspective helps explain the decay results: for the same angular range, longer pendulums store and exchange more energy, so even with comparable dissipation mechanisms, the longer rods take more time to settle. Conversely, shorter pendulums decay more quickly because the energy per cycle is smaller.

Human behavior during active balancing mirrored these mechanical constraints. Participants first trained on the medium pendulum, where performance improved over trials, as evidenced by an increase in time to failure. This suggests that practice improves the control strategy for the medium rod. When subsequently tested on all three rods, there

was no reliable further within-block improvement, but rather the pattern of performance aligned with predictions based on the passive analysis: time to failure was lowest for the short rod, whereas the medium and long rods yielded longer and statistically similar final times to failure. Thus, the intrinsic temporal dynamics of the plant set effective limits on achievable balancing performance, interacting with the inherent sensorimotor delays and noise of the human motor system, even after initial practice had occurred.

Because the medium condition served both as the training condition and as the first testing condition, comparisons involving the medium rod should be interpreted as comparisons with a trained reference condition rather than as fully counterbalanced condition effects. This does not undermine the main contrast between the short and long pendulums, whose order was counterbalanced, but it does mean that the medium-condition performance may partly reflect prior task-specific practice.

The performance effect across pendulum lengths was therefore not explained by a simple monotonic change in maximum cart speed. By the end of testing, estimated maximum cart speed differed significantly across conditions, being highest in the medium condition and lowest in the long condition, with the short condition lying between these values. However, this pattern did not mirror the ordering of time to failure directly. In contrast, estimated peak pendulum angular velocity varied systematically with rod length, being highest for the short rod and lowest for the long rod. This dissociation suggests that while participants adjusted their behavior only modestly across conditions, the mechanical consequences of those actions were strongly shaped by rod length.

Comparisons between training and testing on the medium rod suggest that practice was associated primarily with improved stability rather than with a simple increase in movement speed. A limitation of the current study is that encoder data were acquired at approximately 10 Hz, so derived velocity measures should be interpreted cautiously and primarily as approximate descriptive indicators rather than precise kinematic estimates.

These findings yield two key takeaway messages. First, the present results suggest that practice was not primarily associated with uniformly larger peak movement speeds, but rather with improved performance consistent with adaptation to the system's dynamics. Second, as expected from inverted-pendulum dynamics, longer pendulums are easier to balance than shorter ones because their slower dynamics provide a larger temporal margin for error detection and correction, making the task inherently more forgiving and controllable. In the present data, this was expressed most clearly as a marked difference between the short pendulum and the two longer pendulums, rather than as a fully graded separation between all three conditions.

Relation to previous work

Previous work has emphasized the roles of active feedback and intrinsic passive stiffness in balance maintenance, which is consistent with our observation that both active and passive dynamics contribute to balancing performance (Loram and Lakie, 2002; Lakie et al., 2003; Cabrera and Milton, 2004).

Time-delayed feedback is another central theme in this literature because it complicates balance control and constrains the time available for successful correction. These reaction-time constraints are crucial for balancing performance, and are consistent with the present finding that longer pendulums, which evolve more slowly, were associated with longer times to failure (Kovacs and Insperger, 2022).

Intermittent feedback control, in which active corrections alternate with passive stabilization, has also been proposed as a useful strategy for maintaining stability in inverted pendulum systems and may be relevant to the present findings (Yoshikawa et al., 2016). Related work has shown that intermittent corrections can arise naturally in time-delayed unstable systems (Milton et al., 2009), and skilled stick balancing has likewise been associated with burst-like corrective behavior interspersed with periods of relative inactivity (Cabrera and Milton, 2004).

Interestingly, the present data suggest that participants did not simply scale their control output in direct proportion to pendulum length. Although maximum cart speed differed across conditions, it did not vary monotonically with rod length and therefore did not mirror the ordering of balancing performance directly. In contrast, estimated peak pendulum angular velocity varied systematically across pendulum lengths, with shorter rods showing faster angular motion and longer rods slower angular motion. This pattern is more consistent with the idea that the intrinsic dynamics of the plant, rather than a simple increase in corrective movement speed, played a key role in determining task difficulty. Reaction time delays are known to influence balancing performance, as reflected in our study, where longer pendulums corresponded with longer times to failure.

The present results may also provide insight into human control beyond the general point that performance is better on an easier task. Shortening the pendulum does not simply make the task harder in a nonspecific sense; it increases the intrinsic instability of the plant and reduces the time available for successful correction. The resulting decline in performance is therefore consistent with limits in human sensorimotor control. In particular, the results suggest that participants did not overcome increased instability merely by producing proportionally faster cart movements. Instead, performance appears to have been strongly shaped by the interaction between human sensorimotor constraints and the passive dynamics of the plant. The findings are therefore consistent with the view that balancing performance is limited by constraints within the human sensorimotor

system, including delay, noise, and actuation limits, such that performance deteriorates as task demands increase.

Future work

An important next step will be to compare human performance with that of an optimal computer controller operating on the same task. Such a comparison would provide a useful normative benchmark, helping to distinguish features of performance that arise from the task dynamics themselves from those that reflect biological constraints of the human sensorimotor system. Using the parameters of the pendulums tested here, computational models based on our previous dual linear-quadratic regulator (LQR) framework for this apparatus (Alvarez Hidalgo and Howard, 2022, 2024), could be extended to include sensory delays, signal-dependent noise, friction, and actuation limits. This may help account for empirical features observed in the present study, including the strong effect of pendulum length on time to failure, the systematic variation in pendulum angular velocity across conditions, and the fact that maximum cart speed differed across conditions without mirroring the ordering of balancing performance directly.

A further extension will be to estimate rod-specific pendulum parameters directly from the passive decay trajectories. Building on our previous system-identification approach for the same inverted-pendulum apparatus (Alvarez Hidalgo and Howard, 2024), nonlinear pendulum models will be fitted to the measured oscillatory decay data for each rod length. This will allow effective moment of inertia, viscous damping, and sliding-friction terms to be estimated more directly, rather than relying only on geometric approximations of the rod and pivot assembly. The resulting parameters can then be used to simulate passive fall-to-threshold behavior and to quantify the temporal margins available for human correction in each pendulum condition.

Disclosures

The authors declare that they have no financial, personal, or professional conflicts of interest that may have influenced the content of this paper.

Author Contributions

LAH and ISH conceived the study. LAH implemented the study, conducted data collection, and performed data analysis. The initial draft of the manuscript was written by LAH. Both authors reviewed and edited the manuscript.

Funding Statement
Financial support for LAH was provided by an Engineering and Physical Sciences Research Council (EPSRC) studentship. Institutional support for ISH was provided by the School of Engineering, Computing and Mathematics, University of Plymouth.

Data Availability Statement
Data will be made publicly available upon publication via an online repository (details will be provided upon acceptance).

References

Alvarez Hidalgo L, Howard IS (2022) Gain scheduling for state space control of a dual-mode inverted pendulum. In: 2022 International Conference on System Science and Engineering (ICSSE), pp 039–046. IEEE.

Alvarez Hidalgo L, Howard IS (2024) Dual Mode Control of an Inverted Pendulum: Design, Analysis and Experimental Evaluation. Adv Sci Technol Eng Syst J 8:120–143.

Burdet E, Osu R, Franklin DW, Milner TE, Kawato M (2001) The central nervous system stabilizes unstable dynamics by learning optimal impedance. Nature 414:446–449.

Cabrera JL, Milton JG (2004) Human stick balancing: Tuning Lèvy flights to improve balance control. Chaos Interdiscip J Nonlinear Sci 14:691–698.

Franklin DW, Wolpert DM (2011) Computational mechanisms of sensorimotor control. Neuron 72:425–442.

Gawthrop PJ, Wang L (2006) Intermittent predictive control of an inverted pendulum. Control Eng Pract 14:1347–1356.

Howard I, Ford C, Cangelosi A, Franklin D (2017) Active lead-in variability affects motor memory formation and slows motor learning. Sci Rep 7:7806.

Howard I, Ingram J, Wolpert D (2009) A modular planar robotic manipulandum with end-point torque control. J Neurosci Methods 181:199–211.

Howard IS, Ingram JN, Franklin DW, Wolpert DM (2012) Gone in 0.6 Seconds: The Encoding of Motor Memories Depends on Recent Sensorimotor States. J Neurosci 32:12756–12768.

Howard IS, Wolpert DM, Franklin DW (2013) The effect of contextual cues on the encoding of motor memories. J Neurophysiol 109:2632–2644.

Kovacs BA, Insperger T (2022) Virtual stick balancing: skill development in Newtonian and Aristotelian dynamics. J R Soc Interface 19:20210854.

Krakauer JW, Mazzoni P (2011) Human sensorimotor learning: Adaptation, skill, and beyond. Curr Opin Neurobiol 21:636–644.

Lakie M, Caplan N, Loram ID (2003) Human balancing of an inverted pendulum with a compliant linkage: neural control by anticipatory intermittent bias. J Physiol 551:357–370.

Liu D, Todorov E (2007) Evidence for the Flexible Sensorimotor Strategies Predicted by Optimal Feedback Control. J Neurosci 27:9354–9368.

Loram ID, Lakie M (2002) Human balancing of an inverted pendulum: position control by small, ballistic-like, throw and catch movements. J Physiol 540:1111–1124.

Mehta B, Schaal S (2002) Forward models in visuomotor control. J Neurophysiol 88:942–953.

Milner TE, Franklin DW (2005) Impedance control and internal model use during the initial stage of adaptation to novel dynamics in humans. J Physiol 567:651–664.

Milton J, Cabrera JL, Ohira T, Tajima S, Tonosaki Y, Eurich CW, Campbell SA (2009) The time-delayed inverted pendulum: Implications for human balance control. Chaos Interdiscip J Nonlinear Sci 19:026110.

Oldfield RC (1971) The assessment and analysis of handedness: The Edinburgh inventory. Neuropsychologia 9:97–113.

Scott SH (2004) Optimal feedback control and the neural basis of volitional motor control. Nat Rev Neurosci 5:532–546.

Shadmehr R, Smith MA, Krakauer JW (2010) Error correction, sensory prediction, and adaptation in motor control. Annu Rev Neurosci 33:89–108.

Taylor JA, Ivry RB (2012) The role of strategies in motor learning. Ann N Y Acad Sci 1251:1–12.

Wolpert DM, Diedrichsen J, Flanagan JR (2011) Principles of sensorimotor learning. Nat Rev Neurosci 12:739–751.

Yoshikawa N, Suzuki Y, Kiyono K, Nomura T (2016) Intermittent Feedback-Control Strategy for Stabilizing Inverted Pendulum on Manually Controlled Cart as Analogy to Human Stick Balancing. Front Comput Neurosci 10.